Thermodynamic Modeling and Process Optimization of Supercritical Fluid Fractionation of Fish Oil Fatty Acid Ethyl Esters

S. Espinosa,[†] S. Diaz,[‡] and E. A. Brignole*

Planta Piloto de Ingenieria Quimica, PLAPIQUI (UNS-CONICET), Camino La Carrindanga Km 7, 8000 Bahia Blanca, Argentina

Rigorous thermodynamic modeling, simulation, and optimization of the supercritical fractionation of EPA and DHA esters is presented. These valuable products are obtained from complex mixtures of fish oil fatty acid alkyl esters by high-pressure fractionation with supercritical carbon dioxide. A group contribution equation of state (GC-EOS) that provides reliable phase equilibrium and solubility predictions is used to support the process simulation. A correlation has been developed for the estimation of a thermodynamic model parameter: the fish oil esters hard-sphere diameter. The capability of the group contribution equation of state is confirmed by a detailed comparison of predictions with experimental data. Rigorous simulation models for process units have been formulated within a nonlinear optimization model to maximize EPA and DHA esters recovery and purity from several natural fish oil mixtures with supercritical extraction.

1. Introduction

Fish oils typically contain unsaturated straight-chain fatty acids, ranging from C_{14} to C_{22}, having from one to six double bonds. Fish oil derivatives in the form of ω-3 fatty acids are increasingly demanded as pharmaceutical products, food additives, and health supplements. Among the components of interest are concentrates of EPA (5cis, 8cis, 11cis, 14cis, 17cis eicosapentaenoic acid) and DHA (4cis, 7cis, 10cis, 13cis, 16cis, 19cis docosahexaenoic acid). They have pharmaceutical value in the prevention of atherosclerosis, heart attack, depression, and cancer.[1] Clinical trials have shown that fish oil supplementation is effective in the treatment of many disorders including rheumatoid arthritis[2] and diabetes.

Fish oil fatty acids can be processed either as free fatty acids or as methyl or ethyl esters. Esters are more stable than their respective fatty acids. They are preferred for supercritical fractionation also because of their higher solubility in dense carbon dioxide. The use of ethyl esters is justified in view of methanol toxicity. Different processes have been explored for the fractionation of esters: traditional methods, such as *n*-hexane extraction or vacuum distillation, and novel techniques such as supercritical chromatography,[3] supercritical extraction,[4−7] and extractive urea crystallization.[8] The high degree of unsaturation of these oils precludes the application of vacuum distillation because these components are highly thermally labile. Supercritical chromatography renders high recoveries,[9] but it is only adequate for laboratory-scale operation; Alkio et al.[3] reported the production of EPA and DHA esters with 50% and 90% purity, respectively, from transesterified tuna oil using carbon dioxide as the eluent.

Urea adduction[10] renders fatty acid ethyl esters more concentrated in EPA and DHA than natural ones. In this process, saturated and mono- and diunsaturated fatty acid esters are removed by forming adducts with urea, while more polyunsaturated components remain in the liquid phase and are later fractionated. A 3-fold concentration of EPA and DHA was reported by Borch-Jensen et al.[11] for a urea-fractionated sand eel oil ester. However, the increase in polyunsaturated esters concentration depends on both product recovery and starting oil ester. Urea adduction can be carried out either in organic solvents as ethanol or in supercritical carbon dioxide. The U.S. Food and Drug Administration has recently warned about the formation of a carcinogen, ethyl carbamate, when applying urea adduction with ethanol.[12] Consequently, the use of supercritical carbon dioxide is preferred.[8,13,14]

Selective entrainment (destraction) in supercritical fluids is a feasible alternative for the fractionation of fish oil fatty acid ethyl esters (FAEE) and numerous experimental studies have been reported. Eisenbach[4] showed that EPA could be recovered from a mixture of fatty acid ethyl esters from codfish oil in a semibatch process with supercritical carbon dioxide; he reported 77% EPA recovery with a purity of 48.2%. In this scheme, a hot finger in the top of the column decreases ester solubility in the gas phase working as a partial condenser. Nilsson et al.[6] extended Eisenbach's work and obtained EPA concentrations on the order of 70%, starting from a menhaden oil ester with 75% EPA concentration in the C20 esters fraction. In the same work, these authors also report the supercritical fluid fractionation of a urea-adducted menhaden oil ethyl ester mixture with about 95% EPA concentration in the C20 fraction. They obtained an EPA concentrate of almost 95% purity and a DHA concentrate of more than 90% purity, with 69% and 81% yield, respectively. This work is, to our knowledge, the first one that reports the isolation of EPA and DHA esters with high purity, through fractionation with supercritical carbon dioxide. The semibatch process is adequate for laboratory-scale operation; for large-scale production, the continuous countercurrent process is preferred.[15] Krukonis et al.[16] proposed a two-column scheme and presented simplified

simulation results for the continuous recovery of EPA and DHA from urea-adducted menhaden oil ethyl esters.

Staby and Mollerup[17] made a thorough review on experimental phase equilibrium and solubility data in binary and multicomponent systems of supercritical fluids and fish oils and derivatives; they also reviewed experimental data on supercritical fluid extraction and analytical supercritical fluid chromatography of FAEE. In related studies Staby et al.[18] and Borch-Jensen et al.[11] measured phase equilibrium of supercritical carbon dioxide with natural and urea-adducted fatty acid ethyl esters derived from sand eel oil. Borch-Jensen and Mollerup[19] measured phase equilibrium of polyunsaturated fish oil fatty acids ethyl esters with three different supercritical fluids, carbon dioxide, ethane, and ethylene, at several temperatures and they concluded that the esters were more soluble in ethane than in carbon dioxide at the investigated temperatures.

Coniglio et al.[20] studied phase equilibrium predictions of supercritical carbon dioxide with fish oil derivatives. They explored the combination of the Huron–Vidal[21] first-order (MHV1) and second-order (MHV2)[22] mixing rules to combine the Soave–Redlich–Kwong[23] (SRK) equation of state with different excess Gibbs energy based models such as UNIFAC[24]/UNIQUAC[25] and van der Waals models. They concluded that the MHV1 mixing rules used with modified UNIFAC and a quadratic expression for the co-volume in the equation of state with a universal constant for all systems rendered very satisfactory results.

More recently, Riha and Brunner[26] measured and modeled phase equilibrium of 13 different fatty acid ethyl ester mixtures. Additionally, they performed a continuous fractionation of fatty acid ethyl esters derived from sardine oil with carbon dioxide in a pilot-plant countercurrent destraction column at different operating conditions.[7] Low-molecular-weight components from C14 to C18 were extracted as top product while C20 and C22 (EPA- and DHA-rich esters) constituted the bottom product, and they were obtained with 95% purity and 95% yield. These authors concluded that there is a need for further work on thermodynamic modeling of these multicomponent systems, especially if separation of a real mixture is to be rigorously simulated and optimized.

Diaz et al.[27] have developed nonlinear-programming models for the determination of optimal process schemes and operating conditions in a variety of supercritical fluid processes. Gros et al.[28] and Diaz et al.[29] have formulated mixed-integer nonlinear-programming models for the synthesis and optimization of extraction and dehydration of oxychemicals from aqueous solutions with supercritical fluids. More recently, Espinosa et al.[30,31] have studied the removal of pollutants from fatty oils and the deterpenation of citrus peel oils.

In this work, the application of the Group Contribution Equation of State (GC-EOS)[32–34] has been studied for high-pressure phase equilibria predictions of systems composed of fatty acid ethyl esters and carbon dioxide. Furthermore, optimal schemes and operating conditions for the supercritical fractionation of these esters with carbon dioxide have been determined through the formulation of nonlinear-programming problems that include rigorous models for process units. Different flowsheet alternatives for the fractionation of fish oil ethyl esters have been explored and optimized.

2. Fatty Acids Structure

Fatty acids, naturally found in fats, oils, and lipids, are aliphatic acids with different unsaturation degree. Trivial names, which were often given to long-chain acids before their chemical structure was fully elucidated, frequently refer to the natural source or to the acid physical appearance. Thus, myristic acid was first isolated from seed fats of the Myristiceae and palmitic acid from seed fats of the Palmae. Systematic names, based on IUPAC nomenclature, indicate the chain length of the acid, the position, nature, and configuration of any unsaturated centers, and the position and nature of any substituents. The symbol 18:1 indicates an unbranched C18 acid with one unsaturated center. Because natural polyene acids usually display a common pattern of methylene-interrupted unsaturation, the designation of one double bond also signifies the remainder. Therefore, it is useful to count from the methyl (CH_3) end of the chain. In this way, an acid (or its ester) description is completed with the symbol ωn, where n indicates the first double-bond position in the molecule. According to this nomenclature, eicosapentaenoic acid (EPA) is alternatively referred to as

C20:5 ω3

All cis 5,8,11,14,17 eicosapentaenoic acid (EPA)
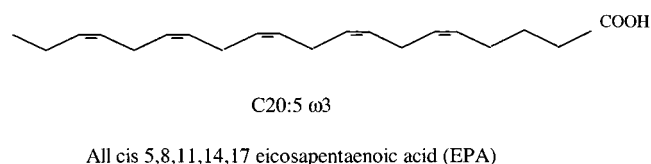
3. Thermodynamic Modeling

Phase equilibrium predictions are made with a group contribution equation of state, GC-EOS, proposed by Skjold-Jørgensen[32,33] to study gas solubility in nonideal mixtures at high pressures. Brignole et al.[35] used this model to predict phase equilibria of mixture components in supercritical fluids. Even though fish oil fatty acids and derivatives are compounds of different chain lengths and degrees of saturation, their molecular structure can be characterized by a few functional groups. The development of supercritical processes for the fractionation of fish oil fatty acids or derivatives requires the prediction of phase equilibrium compositions and conditions for mixtures of high-molecular-weight components with gases at high pressure. The use of the SRK equation or other equations of the van der Waals family have proven to be unsuccessful in correlating and predicting the complex phase equilibrium behavior of triglycerides with near critical fluids. Bottini et al.[36] and Espinosa et al.[37] reported revised sets of parameters for the application of the GC-EOS for natural oils and derivatives. The model is able to describe multicomponent vapor–liquid, liquid–liquid, and liquid–supercritical fluid equilibria with the same parameter set.

In the GC-EOS model, Helmholtz residual energy is expressed as

$$Ar = A_{rep} + A_{att} \tag{1}$$

where A_{rep} (repulsive term) is the free volume contribution and A_{att} is a van der Waals attractive term based on group contribution interactions. The free volume contribution to Helmholtz excess energy is calculated assuming that molecules are hard spheres, so there is a characteristic diameter for each substance. In this way, vapor–liquid equilibrium and liquid–liquid equi-

Table 1. Pure Group Parameters for Fish Oil Fatty Acid Alkyl Esters and Carbon Dioxide for the Group Contribution Equation of State (GC-EOS)[a]

group	T^* (K)	Q	g^*	g'	g''
CO_2	304.2	1.261	531 890	−0.578	0
ester (CH_3COO)	600	1.728	831 400	−1.0930	0
ester (CH_2COO)	600	1.420	831 400	−1.0930	0

[a] T^*, critical temperature of a gas or a reference temperature for a group; q, number of surface segments; g^*, attractive energy parameter [cm^6 atm mol/(surface area segment)^2]; g', g'', linear and logarithmic dependence of energetic parameter with temperature, respectively.

Table 2. Interaction Parameters for Fish Oil Fatty Acid Alkyl Esters and Carbon Dioxide for the Group Contribution Equation of State (GC-EOS)[a]

groups		binary interaction parameters		
i	j	K_{ij}	K'_{ij}	$\alpha_{ij} = \alpha_{ji}$
CH_3COO/CH_2COO	CH_3/CH_2	0.8695	0	0
	$CH{=}CH$	1.006	0	−0.876
	CO_2	1.115	0.094	−1.615

[a] K_{ij}, binary interaction parameter between groups of type j and i; K'_{ij}, temperature dependence of binary interaction parameter; α_{ij}, α_{ji}, nonrandomness parameters.

librium can be predicted for multicomponent systems if hard-sphere diameters for each component are provided, together with interaction parameters for the different groups.

In this work, a strategy is proposed for the determination of hard-sphere diameter for long-chain esters with different unsaturation degrees. Additionally, a discussion on interaction parameter adjustment between groups for mixtures of carbon dioxide and fish oils fatty acid alkyl esters is presented.

3.1. Determination of Interaction Parameters for Fish Oil Fatty Acid Alkyl Esters and Carbon Dioxide. In the GC-EOS model, ester molecules are made up of two different oxygenated groups: CH_3COO- and $-CH_2COO-$. Pure group parameters have been

determined for both groups, as proposed by Fredenslund et al.;[38] they only differ in the number of surface segments/mol (q). Binary interaction parameters with other groups have also been determined. These parameters have been estimated on the basis of experimental information on vapor pressure and vapor−liquid equilibrium data for short-chain esters (methyl and ethyl acetates) with short-chain paraffins, olefins, and carbon dioxide. A detailed description of parametrization can be found in Espinosa et al.[37] Pure group and binary interaction coefficients are presented in Tables 1 and 2.

3.2. Determination of Hard-Sphere Diameter for Fish Oil Fatty Alkyl Esters. The GC-EOS size-related parameter in the repulsive term is the hard-sphere diameter at critical temperature d_c. Skjold-Jørgensen[33] proposes a critical pressure and temperature dependence, $d_c = f(T_c, P_c)$, for gases (composed of only one group, e.g., CO_2) and for molecules with complete randomness ($\alpha_{ij} = 0$ for all i,j, if $v = v_c$). If this is not the case, critical pressure and temperature are not sufficient and the hard-sphere critical diameter is found by matching the calculated and the experimental pure-component vapor pressures, at a given temperature. In this work, hard-sphere diameters for methyl and ethyl esters have been determined this way, when experimental data on vapor pressures are available. However, for many components of the natural fish oil fatty acid esters mixture, vapor pressure data are extremely small and uncertain. In this case, hard-sphere diameters have been adjusted to fit binary vapor−liquid equilibrium for mixtures with carbon dioxide at different temperatures, as has been done to determine critical diameters for EPA and DHA fatty acid esters.

For some esters that compose fish oil FAEE no experimental data on vapor pressure or binary vapor−liquid equilibrium with carbon dioxide are available. In this work, a strategy has been developed to estimate hard-sphere diameter with a correlation based on
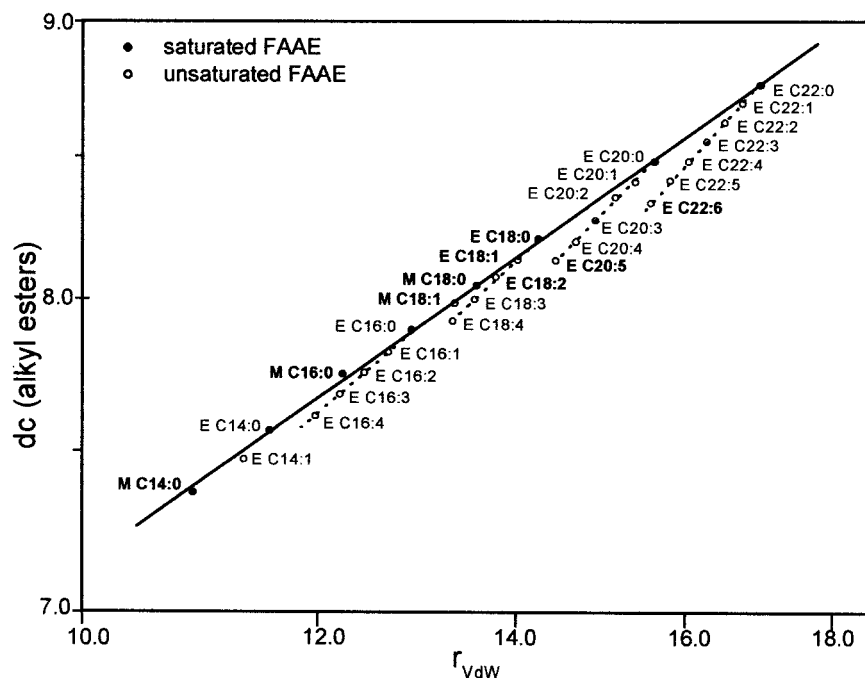

Figure 1. Alkyl esters critical diameter (d_c), as a function of the corresponding van der Waals volume. ●, saturated; ○, unsaturated. −, correlated diameter for saturated alkyl esters. **M**, methyl ester; **E**, ethyl ester. Bold fonts correspond to critical diameters obtained from experimental data.

Table 3. Group Composition (as Modeled with GC-EOS) and Estimated Characteristic Properties for Saturated and Unsaturated Alkyl Esters (M, Methyl Ester; E, Ethyl Ester)

	groups								
component	CH$_3$	CH$_2$	CH=CH	CH$_2$COO	$T_b{}^a$ (K)	$T_c{}^b$ (K)	$P_c{}^b$ (bar)	$r_{VdW}{}^c$	M_w
M C14:0	2	11	0	1	555.43	707.90	14.21	10.897	242
M C16:0	2	13	0	1	585.90	735.40	12.35	12.246	270
M C18:0	2	15	0	1	614.85	762.90	10.84	13.595	298
M C18:1	2	13	1	1	619.33	767.00	10.53	13.363	296
E C14:0	2	12	0	1	570.87	721.67	13.23	11.571	256
E C16:0	2	14	0	1	600.55	749.05	11.56	12.920	284
E C16:1	2	12	1	1	605.17	757.73	11.98	12.688	282
E C16:2	2	10	2	1	609.94	766.94	12.42	12.456	280
E C16:3	2	8	3	1	614.87	776.73	12.89	12.224	278
E C16:4	2	6	4	1	619.98	787.11	13.39	11.991	276
E C18:0	2	16	0	1	628.81	776.70	10.19	14.269	312
E C18:1	2	14	1	1	633.17	784.20	10.53	14.037	310
E C18:2	2	12	2	1	637.67	792.20	10.89	13.805	308
E C18:3	2	10	3	1	642.31	800.70	11.28	13.573	306
E C18:4	2	8	4	1	647.10	809.74	11.69	13.341	304
E C20:0	2	18	0	1	655.80	794.39	9.05	15.618	340
E C20:1	2	16	1	1	659.96	811.44	9.33	15.386	338
E C20:2	2	14	2	1	664.23	818.26	9.64	15.154	336
E C20:3	2	12	3	1	668.62	825.56	9.96	14.922	334
E C20:4	2	10	4	1	673.14	833.33	10.29	14.689	332
E C20:5 (EPA)	2	8	5	1	677.78	878.00	10.64	14.457	330
E C21:5	2	9	5	1	690.30	853.25	10.01	15.132	344
E C22:0	2	20	0	1	681.68	834.65	8.08	16.967	368
E C22:1	2	18	1	1	685.65	839.89	8.33	16.735	366
E C22:2	2	16	2	1	689.72	840.57	8.58	16.502	364
E C22:3	2	14	3	1	693.90	851.67	8.85	16.270	362
E C22:4	2	12	4	1	698.19	858.23	9.13	16.038	360
E C22:5	2	10	5	1	702.59	865.26	9.43	15.806	358
E C22:6 (DHA)	2	8	6	1	707.11	872.77	9.74	15.574	356

^{a} Normal boiling point estimated by the Meissner Method.[31] ^{b} Estimated with the Joback Method.[30] ^{c} r_{VdW}, van der Waals volume, calculated as UNIFAC.[29]

experimental information of homologue compounds. Critical diameters calculated with experimental vapor pressure information have been plotted as a function of the van der Waals volume[38] for each pure ester. In a logarithmic scale, critical diameters for saturated methyl and ethyl esters lie on a straight line, as is shown in Figure 1. In this figure, solid circles represent critical diameters (d_c) for saturated esters; the solid line corresponds to the proposed correlation of d_c as a function of pure esters van der Waals volume (r_{VdW}):

$$\ln(d_c) = 1.075124 + 0.386989 \ln(r_{VdW}) \quad (2)$$

The van der Waals volume for unsaturated esters decreases with the degree of unsaturation. The estimated critical diameter for the unsaturated esters also decreases with the number of CH=CH groups in the molecule. Therefore, to extend the correlation to unsaturated esters, a negative term that depends on the number of (CH=CH) groups should be added,

$$d_c = \exp(1.075124 + 0.386989 \ln(r_{VdW})) - 0.07w \quad (3)$$

where w is the number of (CH=CH) groups in the molecule and r_{VdW} corresponds to the van der Waals volume of the *saturated* ester. In this way, the critical diameter of a polyunsaturated ester such as C20:4 can be calculated with C20:0 van der Waals volume and w = 4. In Figure 1, open circles correspond to critical diameters of unsaturated esters. In the same figure, critical diameters that have been obtained from experimental vapor pressure and VLE data are written in bold font. Critical diameters estimated with eq 3 are written

in regular font. Table 3 shows van der Waals volumes for the esters modeled in this work, together with critical parameters estimated with the Joback method.[39] The corresponding normal boiling point was estimated with the Meissner method.[40]

4. Phase Equilibrium and Solubility Prediction for Fish Oil Fatty Acid Alkyl Esters with Carbon Dioxide

Binary phase equilibrium between pure components and carbon dioxide has been predicted with GC-EOS and compared to experimental data for different methyl esters:[41] myristate (C14:0), palmitate (C16:0), stearate (C18:0), and oleate (C18:1) from 313.15 to 343.15 K and ethyl esters:[42] stearate (C18:0), oleate (C18:1), linoleate (C18:2), eicosapentanoate (C20:5), and docosahexanoate (C22:6), from 313.15 to 333.15 K. Esters group composition is shown in Table 3, together with critical properties, van der Waals volume, and molecular weight. Figures 2−4 compare predictions with experimental information for methyl myristate, EPA, and DHA esters with supercritical carbon dioxide. A good agreement of predictions with experimental values has been found along the entire composition range.

Model predictions have also been tested against experimental phase equilibrium data of several multicomponent mixtures. Riha and Brunner[26] report phase equilibrium measurements for 13 different FAEE mixtures with supercritical carbon dioxide in a temperature range of 313.15−353.15 K and with pressures varying between 9 and 25 MPa. To model these mixtures, they lumped several components into five pseudo-components
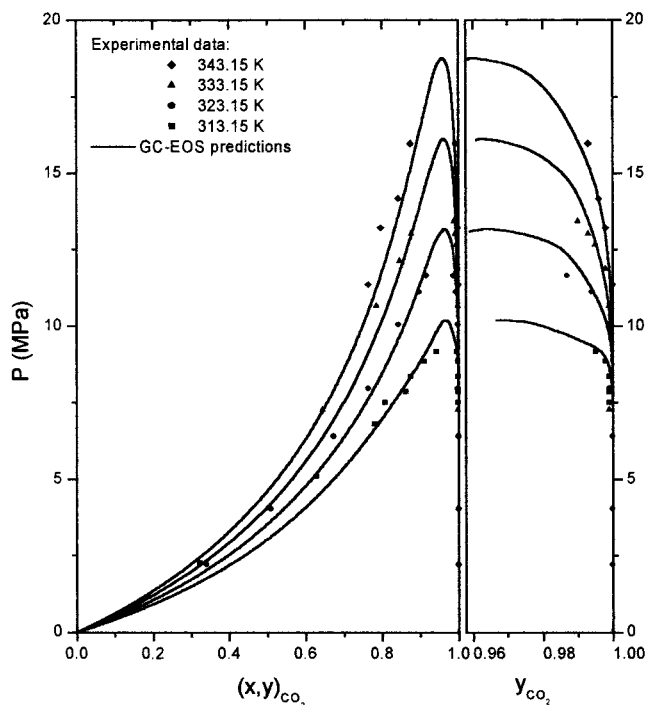
Figure 2. Pressure–composition diagram for the binary system methyl myristate–CO_2. Comparison between GC-EOS predictions and experimental data.[41]
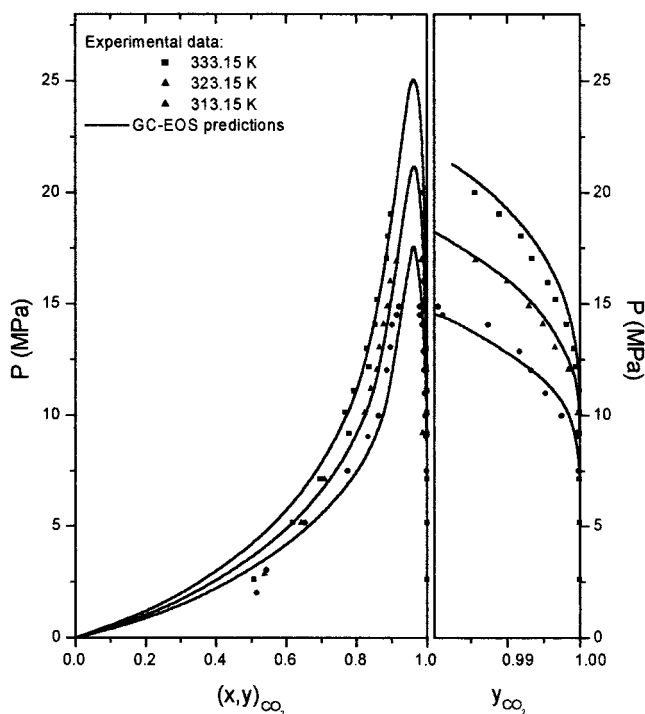

Figure 3. Pressure–composition diagram for the binary system EPA ester–CO_2. Comparison between GC-EOS predictions and experimental data.[42]

Figure 4. Pressure–composition diagram for the binary system DHA ester–CO_2. Comparison between GC-EOS predictions and experimental data.[42]

Table 4. Sardine Oil FAEE Composition; Comparison between EE4 Mixture of Lumped Components[26] and the Five-Component Mixture Modeled with GC-EOS (This Work)

lumped components (experimental data[26])	modeled components (GC-EOS, this work)	mass composition (%)
C14	C14:0	7.69
C16	C16:0	30.73
C18	C18:0	23.25
C20	C20:5	22.55
C22	C22:6	15.78
$M_w = 308.0$	$M_w = 307.3$	

on the basis of chain length (C14, C16, C18, C20, and C22) and they correlated binary and ternary equilibrium data with a cubic equation of state combined with a nonclassic mixing rule. In the present work, the five-component mixture described in Table 4 that represents the EE4 mixture reported by Riha and Brunner[26] has been modeled. The composition of the selected components (C14:0, C16:0, C18:0, C20:5, and C22:6) has been chosen to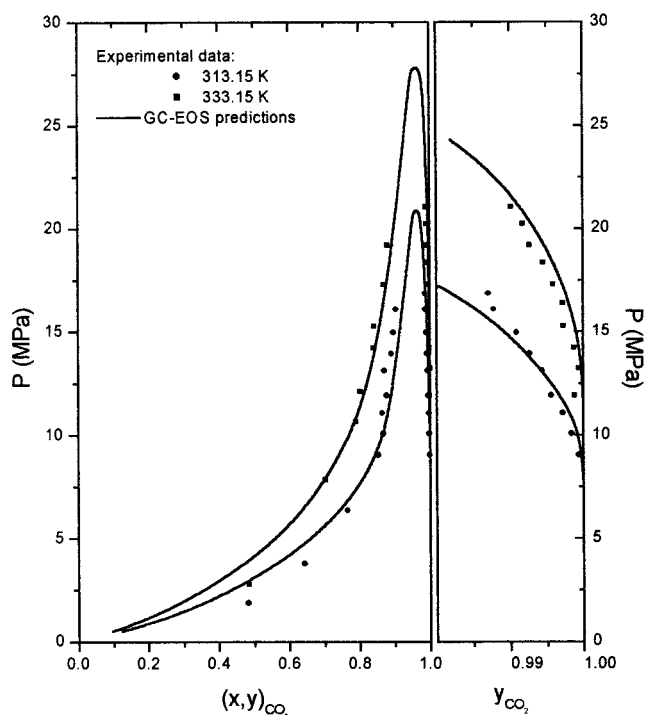 reproduce the molecular weight of the actual mixture (see Table 4). Figure 5 shows the pressure composition diagram for the EE-4 mixture[26] and predictions (this work) at three different temperatures for the five-component mixture with carbon dioxide. Predictions are only based on the group information indicated in Table 3. Furthermore, Figure 6 shows measured and predicted ternary phase equilibrium (C14, C16, C18–C20, C22–CO_2) at 333 K and 14 MPa. Predictions with the group contribution equation of state are in good agreement with experimental data.

A ten-component ω-3 concentrate proposed by Borch-Jensen et al.[11] has also been modeled and vapor–liquid equilibrium predictions of this mixture with carbon dioxide have been compared to experimental data in Figure 7. As can be seen, GC-EOS predictions are satisfactory for 343.15 K but they are not so good at low temperature and at pressure above 8 MPa. Probably, the differences between experimental and predicted liquid-phase compositions are due to the proximity to liquid–liquid equilibrium when the temperature decreases. In this case, the model is very sensitive to the components' critical diameters, some of which have been estimated, as no experimental information was available. However, the enlargement of vapor phase shown on the right side of the figure is in good agreement with experimental data at these temperatures.
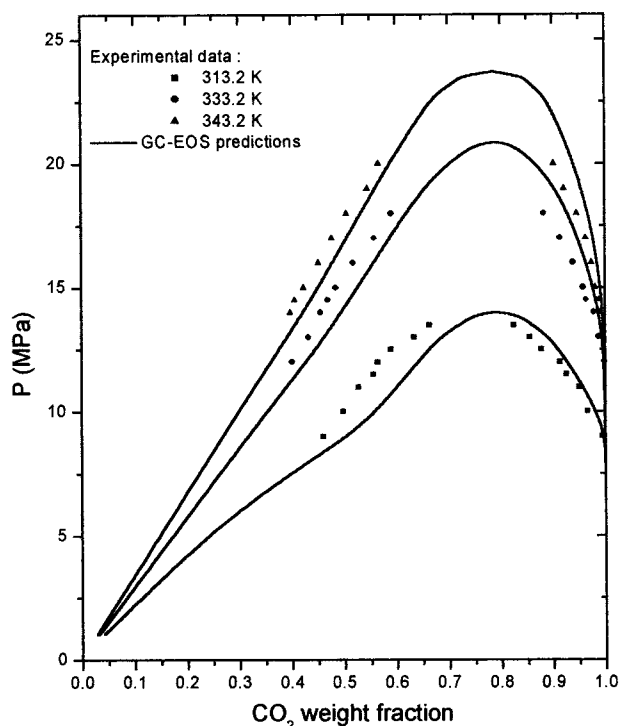
Figure 5. Experimental data[26] (EE-4 mixture) and GC-EOS predictions for CO_2–fatty acid ethyl ester pseudo-binary mixture vapor–liquid equilibrium.
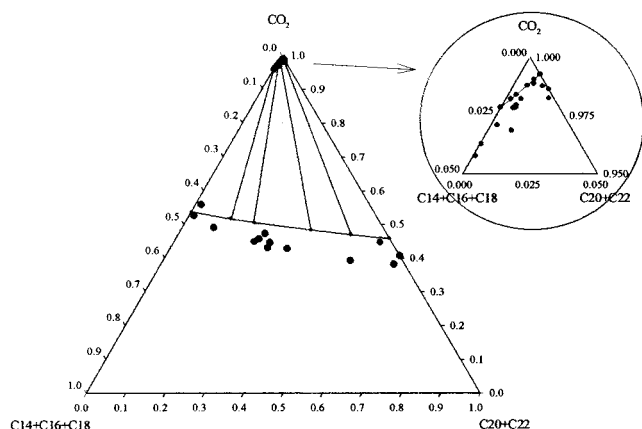

Figure 6. Phase equilibrium (weight fraction) for the pseudo-ternary system at 333.15 K and 14 MPa (weight fraction). ●, experimental data;[26] —, GC-EOS predictions.

Finally, two actual fish oil fatty acid ethyl esters mixtures have been modeled to compare predictions quality with experimental data: a natural sand eel oil ester and a previously urea-adducted one. Table 5 shows these mixtures' composition, as modeled in this work, together with experimental measurements, as determined chromatographically by Staby et al.[18] and Borch-Jensen et al.,[11] respectively. Figure 8 shows the pressure–composition diagram for the natural fish oil ester–CO_2 mixture at 343.15 and 313.15 K. The GC-EOS model predicts conditions of liquid–liquid equilibrium (LLE) at subcritical conditions. Experimental results from Staby et al.[18] report LLE at 283.15 K and the model predicts this behavior at 292.15 K.

Simulation and optimization of extraction processes also require reliable predictions of actual fish oil FAEE solubility and distribution coefficients (K_{FAEE}) in carbon dioxide within the pressure and temperature ranges corresponding to supercritical extraction. In Figure 9,
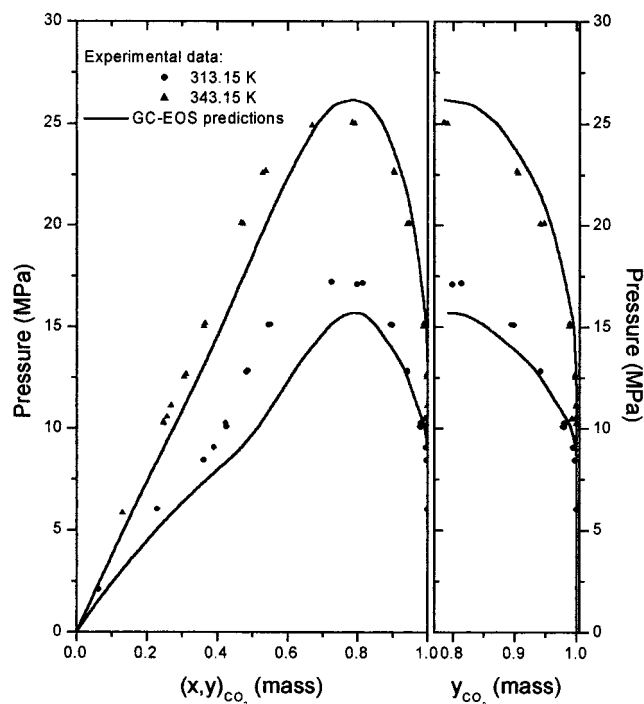

Figure 7. Phase equilibria for an ω-3 concentrate and CO_2. Comparison with experimental data.[11]

experimental data of natural sand eel oil ester solubility in the vapor phase as a function of pressure are compared to GC-EOS predictions for two typical operating temperatures of the fractionation process. In Figure 10, predictions of distribution coefficients for the 13 components that represent the natural sand eel oil ester are plotted against experimental data at 343.15 K and two different pressure levels. Each symbol corresponds to the distribution coefficient of a different ester. The pressure effect on eicosapentaenoic acid (EPA) ester and docosahexaenoic acid (DHA) ester distribution coefficients for the natural sand eel oil ester and carbon dioxide at two different temperatures are shown in Figure 11. This figure confirms that the model is able to predict distribution coefficients for these components at extraction conditions.

Vapor–liquid equilibrium predictions for urea-adducted sand eel oil ester–CO_2 mixtures have also been tested against experimental data. Experimental and predicted distribution coefficients for C14 to C22, on a carbon dioxide free basis, are plotted in Figure 12.

From these results, we can conclude that GC-EOS multicomponent phase equilibrium predictions, based on pure group parameters and interaction coefficients, clearly provide good agreement with experimental data, both for model and actual fatty acid ethyl esters mixtures with supercritical carbon dioxide. With reliable thermodynamic predictions, simulation and optimization of supercritical extraction processes can be performed.

5. Fatty Acid Ethyl Esters Supercritical Fractionation Process
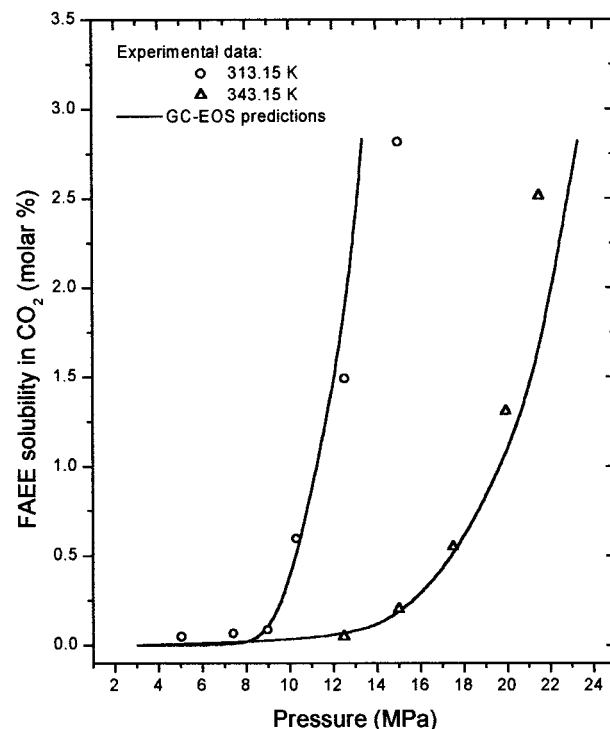
The fractionation of fatty acid ethyl esters, using near critical carbon dioxide, is performed in a high-pressure countercurrent multistage stripping column. A recycle stream of carbon dioxide is fed to the bottom of the column and the components that are more soluble in the carbon dioxide phase are removed from the liquid

Table 5. Sand Eel Oil Esters Composition: Natural[18] and Urea-adducted.[11] Modeled Mixture Composition (GC-EOS) and Experimental Measurements

component	natural sand eel oil		component	urea-adducted sand eel oil	
	exp. data[18] mass %	modeled (this work) mass % (mol %)		exp.data[11] mass %	modeled (this work) mass % (mol %)
C10:0	0.4				
C12:0	0.2				
C14:0	7.5	9.3 (11.1)	C14:0	0.8	1.2 (1.5)
C14:1ω5	0.5		12-Me-C14:0	0.1	
C15:0	0.5		C14:1ω5	0.2	
C15:1ω5	0.2		C15:1ω5	0.1	
C16:0	18.5	18.5 (19.9)	C16:1ω7	0.5	
C16:1ω7	12.4	15.2 (16.5)	14-Me-C16:0	0.3	
C16:2	1.4		C16:2	2.3	3.1 (3.6)
C16:3	0.6		C16:3	1.6	
C16:4ω3	0.8		C16:4ω3	2.9	4.3 (5.1)
C18:0	2.2	2.1 (2.1)			
C18:1ω9	10.2	12.5 (12.2)	C18:1ω9	0.6	
C18:1ω7	2.3		C18:2ω6	1.2	1.8 (1.9)
C18:2ω6	2.9		C18:3ω6	0.8	
C18:3ω6	0.4		C18:3ω3	0.9	1.7 (1.8)
C18:3ω3	1.3	8.4 (8.4)	C18:4ω3	12.7	12.5 (13.5)
C18:4ω3	3.8				
C20:0	0.2		C20:1ω9	0.6	
C20:1ω9	4.2	4.4 (4.0)	C20:2ω6	0.5	1.1 (1.1)
C20:2ω6	0.3		C20:4ω6	0.9	
C20:3ω3	0.2		C20:3ω3	0.1	
C20:4ω3	0.7	1.2 (1.1)	C20:4ω3	1.0	1.8 (1.8)
C20:5ω3 (EPA)	10.0	10.1 (9.3)	C20:5ω3 (EPA)	35.9	35.9 (35.8)
C22:1ω11	6.5	7.6 (6.3)	C22:1ω11	0.3	0.4 (0.4)
C22:1ω9	1.0		C22:1ω9	0.1	
C21:5ω3	0.4	0.5 (0.4)	C21:5ω3	1.5	1.5 (1.4)
C22:5ω3	0.5	0.5 (0.4)	C22:5ω3	0.4	1.5 (1.4)
C22:6ω3 (DHA)	9.6	9.7 (8.3)	C22:5ω6	1.1	
			C22:6ω3 (DHA)	33.2	33.2 (30.7)
percent EPA in C20 esters		*64.5*	percent EPA in C20 esters		*92.0*
percent DHA in C22 esters		*53.9*	percent DHA in C22 esters		*90.7*
M_w	*305.18*	*304.83*	M_w	*328.60*	*328.69*
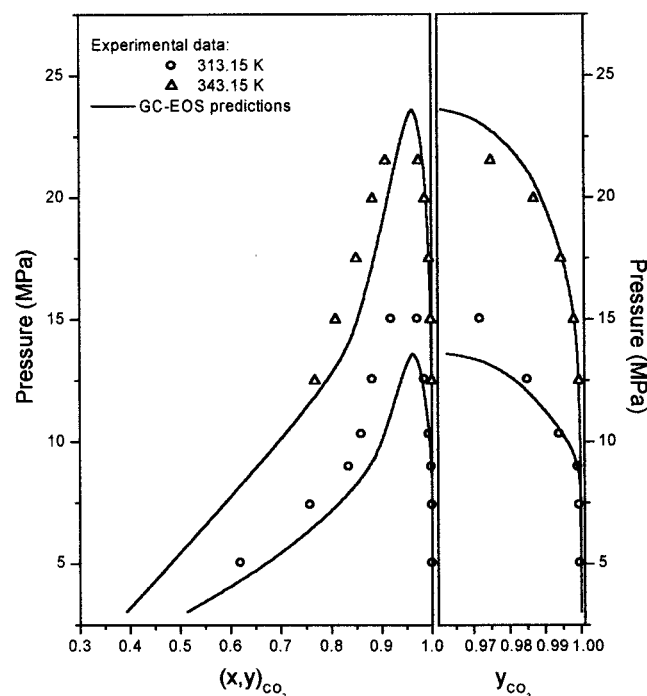
Figure 8. Pressure–composition diagram for a natural sand eel oil ester mixture and CO_2. Experimental values[18] and GC-EOS predictions (this work).

Figure 9. Solubility of natural fish oil ester in CO_2 as a function of pressure, at two different temperatures. Comparison between experimental[18] and predicted values (this work).

phase. The FAEE feed is introduced at an intermediate position. The top gas, rich in the more volatile components, is heated and expanded into a separator vessel. Under these conditions, fatty acid ethyl esters solubility in the carbon dioxide phase is drastically reduced and they form a saturated liquid phase. Carbon dioxide is recompressed and recycled to the column. The liquid is
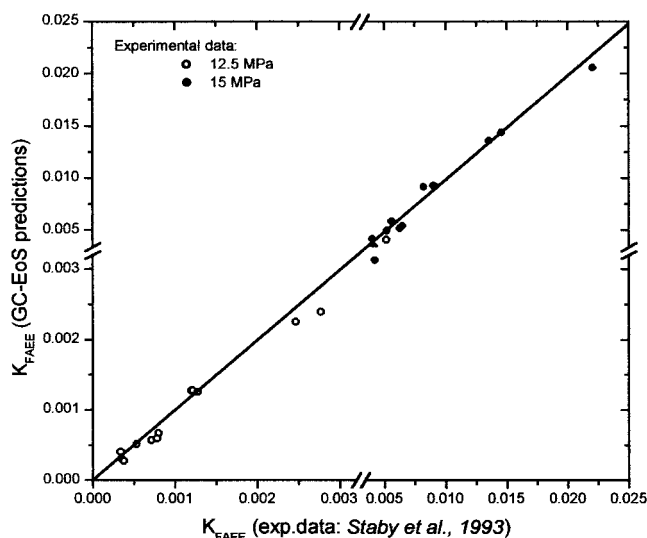
Figure 10. Natural sand eel oil esters distribution coefficients (K_{FAEE}). Comparison between predictions and experimental data[18] at 12.5 and 15 MPa.
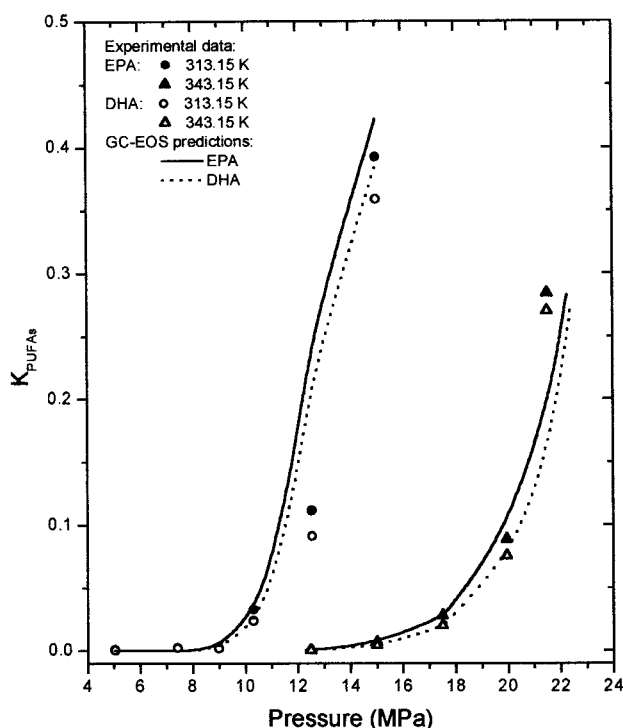

Figure 11. Pressure dependence of EPA and DHA esters distribution coefficients between a natural sand eel oil ester[18] and CO_2 at two temperatures.

partly returned as reflux to the column and the rest is obtained as distillate. The raffinate is a stream of FAEE enriched in heavier components. Even though the reflux has a rectification effect, it is mainly needed to keep the system within the two-phase region. Additional columns are required to complete the FAEE fractionation. Figure 13 shows a three-column scheme to produce EPA and DHA esters product streams.

6. Simulation and Optimization Model

The optimization problem for the determination of optimal operating conditions for different supercritical process schemes has been formulated as the following
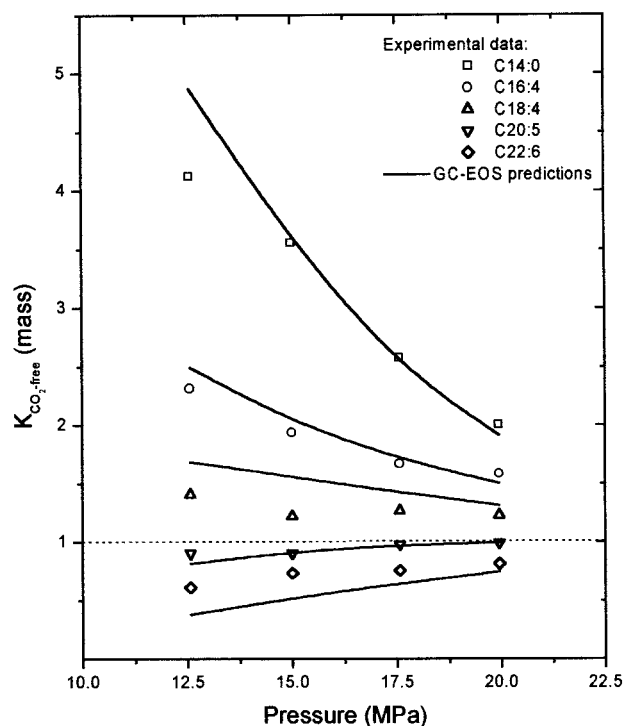

Figure 12. Distribution coefficients, on a CO_2-free basis, of C14–C22 ethyl esters from a urea-adducted fish oil, at 343.15 K, as a function of pressure. Experimental data[11] and GC-EOS predictions (this work).

nonlinear-programming (NLP) model:

$$\text{Max } f(x)$$

$$x$$

$$\text{s.t.}$$

$$h(x) = 0$$

$$c(x) = 0$$

$$g(x) \leq 0$$

$$x \in 2^n, \quad x_L \leq x \leq x_U$$

where x corresponds to optimization variables, which have been selected to represent main continuous decisions. They are extraction pressure and temperature, solvent flow rate, and reflux ratio for each extraction–separation stage. Equality constraints, h, represent the process mathematical model that is solved within a sequential process simulator. This program includes rigorous models for a high-pressure multistage extractor[34] and a multiphase flash.[43] The GC-EOS has been integrated as thermodynamic support for these model unit simulation routines. Inequality constraints, g, include process specifications and operating bounds. In this work, the objective function is the maximization of EPA (C20:5) and DHA (C22:6) esters recovery. Additional equality constraints c correspond to reflux recycle equations, as the nonlinear optimization subproblem has been solved in an infeasible-path way. Nonlinear-programming problems have been solved with a Successive Quadratic Programming algorithm.[44] The nonlinear optimization model, solved with local optimization techniques, does not guarantee solution to global optimality. However, reported numerical results
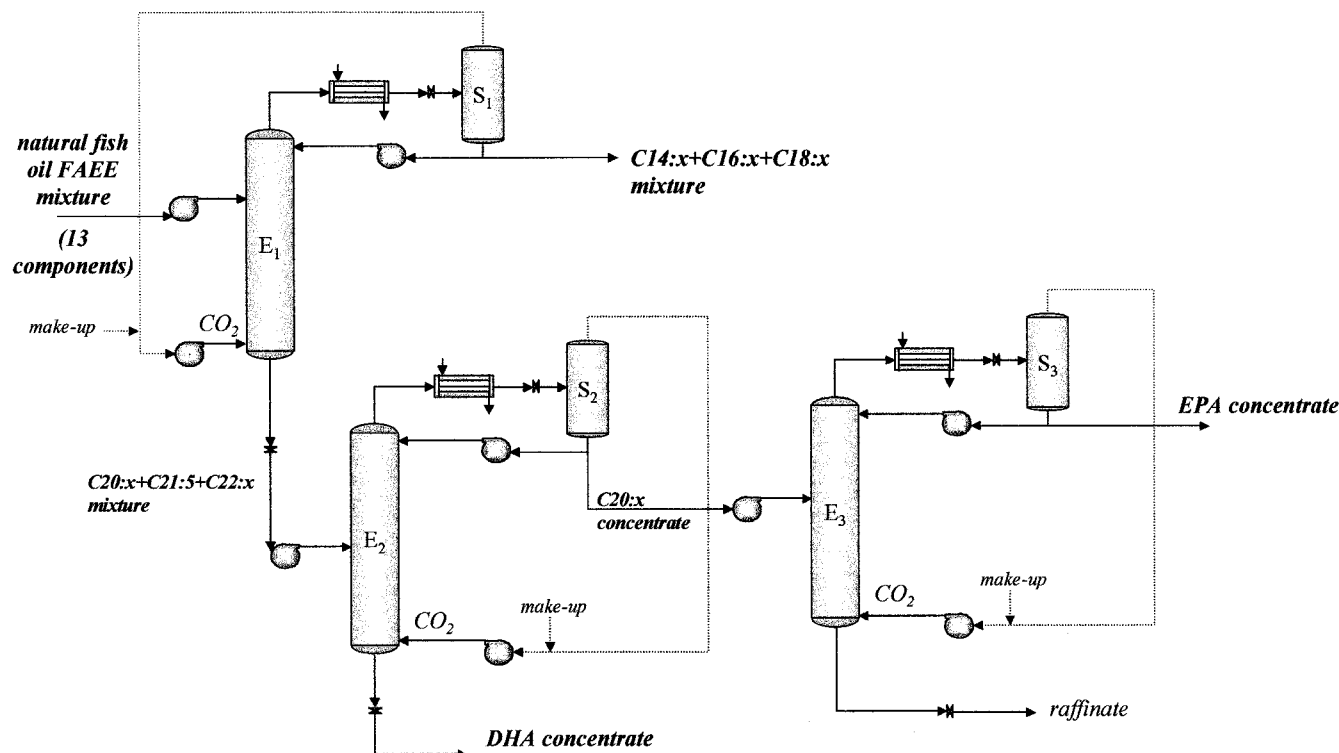
Figure 13. Three-column scheme for the fractionation of EPA and DHA esters with supercritical carbon dioxide from natural sand eel oil.

Table 6. Fractionation of Sardine Oil Ester with Supercritical Carbon Dioxide; Experimental[7] and Simulation Results (This Work)

variables	experimental value	simulation results
pextractor (MPa)	14.5	14.5
textractor (K)	333.15	333.15
reflux to column/condensed top liquid	0.88	0.74
solvent/feed (wt)	126.00	102.67
top product purity (C14, C16, C18) (wt %)	95.98	97.61
bottom product purity (%)	99.04	99.32
C14−18 recovery (%)	99.40	99.20
C20−22 recovery (%)	92.66	95.24

have been obtained running the program with different initial points that converged to the same local optimum.

7. Discussion of Results

7.1. Separation of C20+ and C18− Fractions from a Sardine Oil Ester Mixture. Process Simulation: Comparison to Pilot-Plant Results (Riha and Brunner[7]). A simple extractor−separator system has been rigorously simulated for the conditions of pilot-plant studies reported by Riha and Brunner.[7] These authors performed the separation between the low-molecular-weight esters (C14, C16, and C18) and the high-molecular-weight ones (C20 and C22) in a pilot-plant countercurrent destraction column. A concentrate of the mixture of C20 and C22 esters was obtained as the bottom product processing a sardine oil ester mixture. The feed mixture composition is described in Table 4. The same operating conditions have been simulated for a 40-stages column and Table 6 shows a comparison between simulation results and experimental values reported by Riha and Brunner.[7] The agreement is quite good considering that the relative volatility between the key components is <1.5 and, in this range, separation process variables are very sensitive to errors in relative volatility.

7.2. Process Optimization for EPA and DHA Esters Recovery from Actual FAEE Mixtures. 7.2.1. EPA and DHA Esters Recovery. Supercritical Carbon Dioxide Fractionation. A nonlinear-programming model has been formulated to determine optimal operating conditions for the supercritical fractionation of a natural sand eel oil ester to obtain EPA and DHA esters concentrate streams. The feed chromatographic composition has been taken from Staby et al.[18] (see Table 5) and it has been modeled as a 13-component mixture in which fatty acid ethyl esters range from C14:x to C22:x (section 4). Several compounds of the same carbon number were included to explore the possibility of separating EPA and DHA from FAEE of similar carbon number. Figure 13 shows the analyzed three-column fractionation process. In the first column, an enriched mixture of C20:x to C22:x components is obtained as the bottom product. The destraction process is mainly a stripping process with only a minor rectification effect. Therefore, it is possible to obtain a clear cut regarding the removal of light components from the bottom product of each column, but the top product is always contaminated with components of higher carbon number. This effect can also be observed from pilot-plant and simulation results reported in Table 6. Therefore, some EPA ester is lost in the first column and some DHA ester in the top product of the second. In this column, DHA ester is obtained as bottom product, and in the third one, an EPA concentrate is recovered as the distillate.

Table 7 shows bounds on optimization variables and their values at the nonlinear-programming optimum for each column. The reflux ratio corresponds to the fraction of the liquid product that is recycled to the extraction column. The columns operate at similar temperatures, but higher pressures are required for the last two columns. These two columns require higher solvent-to-

Table 7. Main Optimization Variables and Their Bounds for the Recovery of EPA and DHA Esters with Supercritical Carbon Dioxide in the Three-Column Scheme Optimum (Feed: Natural Sand Eel Oil Ester (Table 4))

			operating optimum		
variable	lower bound	upper bound	column E1	column E2	column E3
pextr (MPa)	12.00	17.00	14.50	15.52	15.80
textr (K)	320.00	350.00	333.02	333.30	334.60
reflux (%)	40.00	90.00	77.00	79.00	83.00
solvent/feed (mass basis)	100.00	300.00	110.21	193.85	208.55

Table 8. Optimal Overall Product Recovery and Purity for a Three-Column Separation Scheme with Carbon Dioxide (Feed: Natural Sand Eel Oil Ester)

variable	operating optimum
C20 overall recovery (%)	93.72
C20 in product stream (mol %)	91.70
EPA overall recovery (%)	94.98
EPA in product stream (mol %)	60.46
DHA overall recovery (%)	80.02
DHA in product stream (mol %)	80.09

Table 9. Individual Unit Detail of Product Recovery and Concentration for the Fractionation of Natural Sand Eel Oil FAEE with Carbon Dioxide in the Three-Column Scheme Optimum (T: Top Product; B: Bottom Product)

variable	column E1	column E2	column E3
number of stages	40	48	60
feed plate	12	24	25
C14−C18 recovery (%)	99.7 (T)	100.00 (T)	
C20 recovery (%)	96.28 (B)	99.90 (T)	97.44 (T)
C20 concentration (mol %)	47.04 (B)	65.47 (T)	91.70 (T)
EPA recovery (%)	96.82 (B)	99.92 (T)	98.18 (T)
EPA concentration (mol %)	30.88 (B)	42.97 (T)	60.46 (T)
C22 recovery (%)	99.87 (B)	55.46 (B)	90.63 (B)
C22 concentration (mol %)	50.83 (B)	99.83 (B)	94.46 (B)
DHA recovery (%)	99.97 (B)	80.34 (B)	99.63 (B)
DHA concentration (mol %)	28.15 (B)	80.09 (B)	25.40 (B)

feed ratios than the first one because the separation takes place among components in a narrower carbon range (C20 + C21 + C22). Table 8 gives optimal overall product recovery and purity. An EPA ester concentrate (60.46 mol %) has been obtained as product stream (top product in column E3); however, C20 ester concentration in this stream is 91.70 mol %. This is due to the low EPA concentration in the C20 fraction of the natural sand eel oil ester feed (64.50 mol %, see Table 5). This indicates that no further separation could be obtained in this column between EPA and the remaining C20 esters. Table 8 also shows that optimal DHA overall recovery has been 80.02% in the product stream (bottom stream in column E2), with about 80 mol % concentration, and 99.83% C22 esters fraction concentration. The remaining DHA and C22 esters have been obtained as bottom product in the third column. Product recovery and stream composition for the different columns that comprise the entire separation scheme are given in Table 9.

The addition of an entrainer to further fractionate fatty acid ethyl esters, of a given carbon number, on the basis of the different unsaturation degree has also been explored. Numerical results indicate that even though the addition of ethyl acetate increases esters solubility in the vapor phase, it is not selective on the unsaturation degree. For example, a DHA product stream (E2 bottoms) has been further fractionated in a fourth column with supercritical carbon dioxide and ethyl acetate (<1% ethyl acetate in carbon dioxide), but DHA

recovery could not be improved. The same conclusion was obtained when exploring the use of this entrainer in an additional column to separate EPA from the rest of C20 fatty acid ethyl esters.

Numerical results show that supercritical carbon dioxide fractionation can be comparable to one step of supercritical chromatography that renders 50 and 90% EPA and DHA esters concentrates from tuna oil ester.[3] It is important to note that tuna oil has a higher DHA content than sand eel oil (24 vs 11%).

7.2.2. EPA and DHA Esters Recovery. Supercritical Fractionation Combined with Urea Adduction. EPA and DHA esters concentrations in product streams are strongly dependent on their concentration in C20 and C22 fractions in the feed. Esters of the same carbon number have relative volatilities close to 1 and simulation results indicate that they cannot be separated with supercritical fractionation. If the starting fish oil ester contains a higher concentration of EPA and DHA, higher product purity can be expected. The urea-adduction technique provides a concentrate of polyunsaturated esters. In this technique, the esters are mixed with a hot solution of urea in a solvent such as ethanol. After cooling, urea crystallizes, forming adducts with saturated esters and mono- and dienes while polyunsaturated fatty acid esters remain dissolved and they can be later isolated from the solvent phase.

Process optimization has been performed for the urea-adducted sand eel oil ester whose chromatographic composition was reported by Borch-Jensen et al.;[11] this mixture has been modeled as a 13-component one, as is shown in Table 5 (sixth column). Predictions of the feed mixture distribution coefficient between the liquid phase and supercritical carbon dioxide are compared to experimental values in Figure 12, on a carbon dioxide free basis.

In a two-column scheme, 92.2% EPA ester can be recovered as top product in the second column, with only 74.71% EPA ester concentration. Consequently, a third column is required, rendering the process scheme shown in Figure 14, where the third-column raffinate is EPA ester product stream. In this case, the process has an optimal overall EPA recovery of 80.18% with 80% EPA molar concentration in column E3 raffinate (versus 60% when it is obtained from natural sand eel oil). Column E2 bottom product is a DHA concentrate, 95.32 mol % concentration, with an overall DHA recovery of 89.06%. Tables 10−12 show the main operating variables, solvent-to-feed ratio, and product recoveries in this process optimum.

In the supercritical fractionation of natural sand eel oil ester (without urea adduction), a clear cut is obtained between C18 and C20 in the first destraction column. However, with urea adduction, the separation between C18 and C20 is very difficult, so C20 recovery is 92.5% in the raffinate, with 86% C18 recovery in the top product stream (versus 99% in the natural oil ester fractionation).

Front-end urea adduction in fish oil fatty acid ethyl esters mixtures improves product purity. However, simulation results show that feed pretreatment makes esters separation in the first destraction column rather difficult: C18 distributes between extract and raffinate and it must be obtained as top product in the third column, with a consequent 20% EPA ester loss in the lighter fraction. An alternative to obtain higher purity products with higher recovery can be the introduction
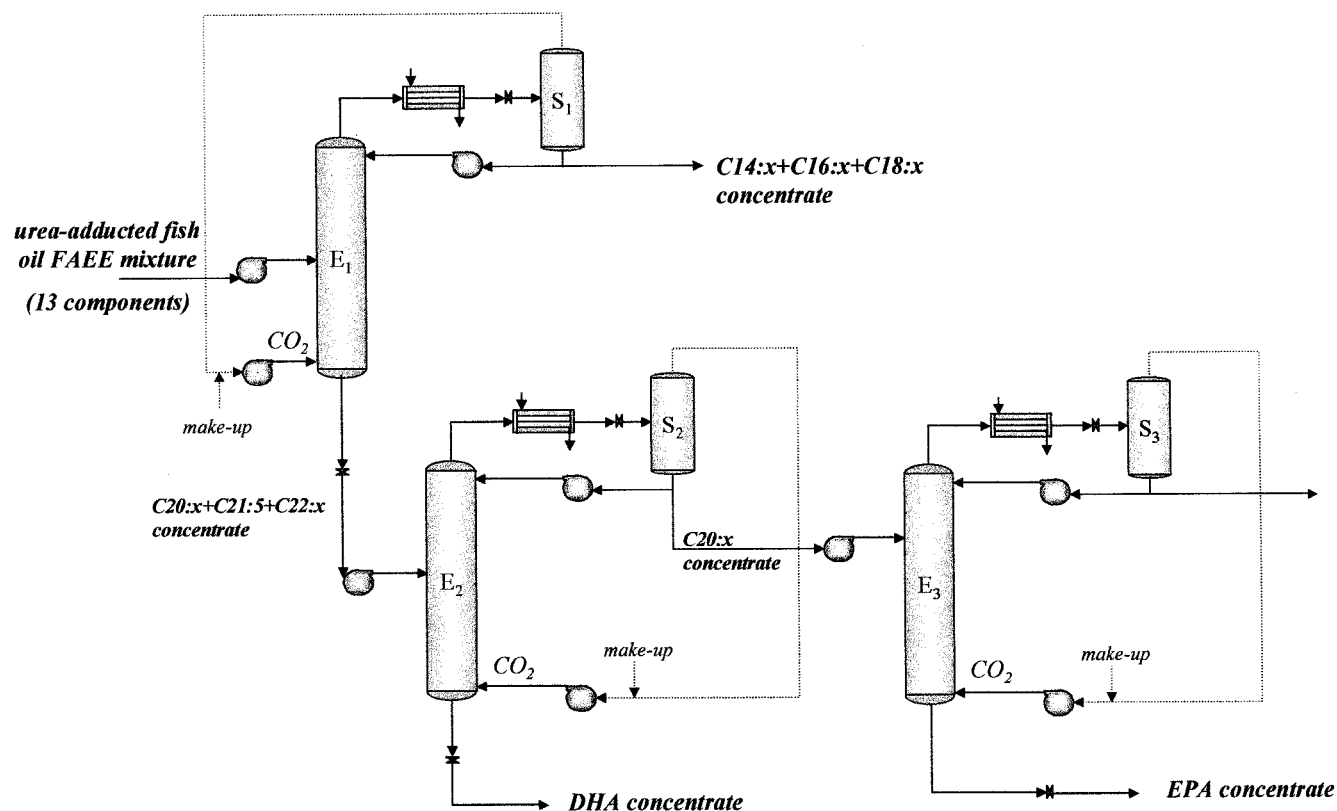
Figure 14. Recovery of EPA and DHA esters from a urea-adducted fish oil FAEE mixture with supercritical carbon dioxide.

Table 10. Main Optimization Variables and Their Bounds for the Recovery of EPA and DHA Esters Concentrate with Supercritical Carbon Dioxide in the Three-Column Scheme Optimum (Feed: Urea-Adducted Sand Eel Oil)

variable	lower bound	upper bound	operating optimum column E1	operating optimum column E2	operating optimum column E3
pextr (MPa)	12.00	17.00	15.9	15.84	14.99
textr (K)	320.00	350.00	340.3	334.8	339.5
reflux (%)	40.00	90.00	83.0	78.9	87.8
solvent/feed (mass basis)	100.00	300.00	90.5	147.87	174.30

Table 11. Optimal Overall Product Recovery for a Three-Column Separation Scheme with Carbon Dioxide (Feed: Urea-Adducted Sand Eel Oil)

variable	operating optimum
C20 overall recovery (%)	83.35
C20 in product stream (mol %)	86.37
EPA overall recovery (%)	80.18
EPA in product stream (mol %)	80.00
DHA overall recovery (%)	89.06
DHA in product stream (mol %)	95.32

of a urea-adduction step for each product stream at the end of the supercritical carbon dioxide fractionation process in Figure 13. In this way, EPA ester concentration in the product stream can increase from 60 to 87% and DHA ester concentration can become up to 96% in product stream, if all saturated esters, monoenes, and dienes could be removed from the product streams. However, product recovery decreases, depending on the efficiency of the urea-adduction process.

Finally, the use of a urea-adduction step after column E1 in Figure 13 (the raffinate is a 59.03% EPA−DHA esters concentrate) could render a 90.50% EPA−DHA esters concentrate. This stream can be either delivered

Table 12. Individual Unit Detail of Product Recovery and Concentration for the Fractionation of Sand Eel Oil FAEE with Carbon Dioxide in the Three-Column Scheme Optimal Operating Point (T: Top Product; B: Bottom Product)

variable	column E1	column E2	column E3
number of stages	60	60	40
feed plate	30	25	6
C14−C18 recovery (%)	86.06 (T)	100.00 (T)	90.52 (T)
C20 recovery (%)	92.50 (B)	99.61 (T)	90.46 (B)
C20 concentration (mol %)	48.70 (B)	80.68 (T)	86.37 (B)
EPA recovery (%)	92.49 (B)	99.67 (T)	86.98 (B)
EPA concentration (mol %)	45.10 (B)	74.71 (T)	80.00 (B)
C22 recovery (%)	100.00 (B)	89.81 (B)	99.16 (B)
C22 concentration (mol %)	44.16 (B)	99.52 (B)	9.14 (B)
DHA recovery (%)	100.00 (B)	90.89 (B)	99.38 (B)
DHA concentration (mol %)	41.79 (B)	95.32 (B)	7.75 (B)

as a high-purity $\omega 3$ concentrate or be further fractionated in columns E2 and E3.

Conclusions and Summary

Accurate predictions of phase equilibria for mixtures of highly unsaturated mixtures of fish oil fatty esters in mixtures with carbon dioxide at near critical conditions have been obtained with the GC-EOS thermodynamic model. A group contribution correlation of critical diameters has been developed for components for which no experimental information is available. Rigorous simulations and predictions are validated with experimental results. The formulation of a nonlinear-programming model allows the determination of optimal conditions for complex destraction columns, highly sensitive to the operating reflux, carbon dioxide flow rate, pressure, and temperature. Processing schemes for different natural fish oil ester mixtures are discussed. Process simulations and thermodynamic predictions justify the use of urea-adduction steps if high concentration and recovery of EPA and DHA esters are required.

Acknowledgment

Literature Cited

(1) Fats and Oils in Human Nutrition. Report of a Joint Expert Consultation. In *FAO Food Nutr. Pap. Ser.* **1998**, *57*.

(2) Kremer, J. M. ω-3 Fatty Acid Supplements in Rheumatoid Arthritis. *Am. J. Clin. Nutr.* **2000**, *71* (suppl), 349s.

(3) Alkio, M.; Gonzalez, C.; Jantii, M.; Aaltonen, O. Purification of Polyunsaturated Fatty Acid Esters from Tuna Oil with Super-critical Fluid Chromatography. *J. Am. Oil Chem. Soc.* **2000**, *77* (3), 315.

(4) Eisenbach, W. Supercritical Fluid Extraction: A Film Demonstration. *Ber. Bunsen-Ges. Phys. Chem.* **1984**, *88*, 882.

(5) Krukonis, V. J. Processing with Supercritical Fluids. Overview and Applications. In *Supercritical Fluid Extraction and Chromatography*; ACS Symposium Series 366; B. A. Charpentier and M. R. Sevenants, Eds.; American Chemical Society: Washington, DC, 1988; p 26.

(6) Nilsson, W. B.; Gauglitz, E.; Hudson, J.; Stout, J.; Spinelli, J. Fractionation of Menhaden Oil Ethyl Esters using Supercritical Fluid CO₂. *J. Am. Oil Chem. Soc.* **1988**, *65* (1), 109.

(7) Riha, V.; Brunner, G. Separation of Fish Oil Ethyl Esters with Supercritical Carbon Dioxide. *J. Supercrit. Fluids* **2000**, *17*, 55.

(8) Arai, K.; Saito, S. Fractionation of Fatty Acids and their Derivatives by Extractive Crystallization using Gas as a Solvent, World Congress III of Chemical Engineering, Tokyo, 1986.

(9) Nilsson, W. B. Supercritical Fluid Extraction and Fractionation of Fish Oils. In *Supercritical Fluid Technology in Oils and Liquids Chemistry*; King, J., List, G., Eds.; AOCS Press: Champaign, IL, 1996; Chapter 8.

(10) Schlenk, H.; Holman, R. Separation and Stabilization of Fatty Acids by Urea Complexes, *J. Am. Chem. Soc.* **1950**, *72*, 5001.

(11) Borch-Jensen, C.; Staby, A.; Mollerup, J. Phase Equilibria of Urea-Fractionated Fish Oil Fatty Acid Ethyl Esters and Supercritical Carbon Dioxide. *Ind. Eng. Chem. Res.* **1994**, *33*, 1574.

(12) Canas, B.; Yurawecz, M. Ethyl Carbamate Formation During Urea Complexation for Fractionation of Fatty Acids. *J. Am. Oil Chem. Soc.* **1999**, *76*, 537.

(13) Saito, S. Supercritical Gas Extraction of Food and Natural Products II. Applications to Condensation of Ethanol and to Separation of Polyunsaturated Fatty Acids. *Kagaku Seibutsu* **1986**, *24*, 201.

(14) Suzuki, Y.; Konno, M.; Arai, K.; Saito, S. Fractionation of Polyunaturated Fatty Acids by Urea Adduct Formation using Supercritical Fluid CO₂ as Solvent. *Kagaku Kogaku Ronbunshu* **1990**, *16*, 38.

(15) Brunner, G. *Gas Extraction. An Introduction to Fundamentals of Supercritical Fluids and the Application to Separation Processes*; Springer: New York, 1994.

(16) Krukonis, V. J.; Vivian, J.; Bambara, C.; Nilsson, W.; Martin, R. Concentration of Eicosapentaenoic Acid by Supercritical Fluid Extraction: A Design Study of a Continuous Production Process. In *Advances in Seafood Biochemistry, Composition and Quality*; Papers from the ACS Annual Meeting, New Orleans, LA; Flick, G., Martin, R., Eds.; American Chemical Society: Washington, DC, 1992; p 169.

(17) Staby, A.; Mollerup, J. Separation of Constituents of Fish Oil using Supercritical Fluids: A Review of Experimental Solubility, Extraction and Chromatographic Data. *Fluid Phase Equilibr.* **1993**, *91*, 349.

(18) Staby, A.; Forskov, T.; Mollerup, J. Phase Equilibria of Fish Oil Fatty Acid Ethyl Esters and Sub- and Supercritical CO₂. *Fluid Phase Equilibr.* **1993**, *87*, 309.

(19) Borch-Jensen, C.; Mollerup, J. Phase Equilibria of Long-Chain Polyunsaturated Fish Oil Fatty Acid Ethyl Esters and Carbon Dioxide, Ethane or Ethylene at Reduced Gas Temperatures of 1.03 and 1.13. *Fluid Phase Equilibr.* **1999**, *161*, 169.

(20) Coniglio, L.; Knudsen, K.; Gani, R. Model Prediction of Supercritical Fluid-Liquid Equilibria for Carbon Dioxide and Fish Oil Related Compounds. *Ind. Eng. Chem. Res.* **1995**, *34*, 2473.

(21) Huron, M. J.; Vidal, J. New Mixing Rules in Simple EOS for Representing VLE of Strongly Non-ideal Mixtures. *Fluid Phase Equilibr.* **1979**, *3*, 255.

(22) Michelsen, M. L. A Method for Incorporating Excess Gibbs Energy Models in Equations of State. *Fluid Phase Equilibr.* **1990**, *60*, 42.

(23) Soave, G. Equilibrium Constants from a Modified Redlich-Kwong Equation of State. *Chem. Eng. Sci.* **1972**, *27*, 1197.

(24) Fredenslund, Aa.; Jones, R. L.; Prausnitz, J. M. Group-Contribution Estimation of Activity Coefficients in Nonideal Liquid Mixtures. *AIChE J.* **1975**, *21*, 1086.

(25) Abrams, D.; Prausnitz, J. Statistical Thermodynamics of Liquid Mixtures: A New Expression for the Excess Gibbs Energy of Partly or Completely Miscible Systems. *AIChE J.* **1975**, *21*, 116.

(26) Riha, V.; Brunner, G. Phase Equilibria of Fish Oil Ethyl Esters with Supercritical Carbon Dioxide. *J. Supercrit. Fluids* **1999**, *15*, 33.

(27) Diaz, S.; Espinosa, S.; Brignole, E. A. Modeling and Simulation Tools for Supercritical Fluid Processes. *Comput.-Aided Process Eng.* **2000**, *8*, 319.

(28) Gros, H.; Diaz, S.; Brignole, E. A. Process Synthesis and Optimization of Near Critical Separations of Aqueous Azeotropic Mixtures. *J. Supercrit. Fluids* **1998**, *12*, 69.

(29) Diaz, S.; Gros, H.; Brignole, E. A. Thermodynamic Modeling, Synthesis and Optimization of Extraction-Dehydration Processes. *Comput. Chem. Eng.* **2000**, *24* (9), 2069.

(30) Espinosa, S.; Bottini, S.; Brignole, E. A. Process Analysis and Phase Equilibria for the Removal of Chemicals from Fatty Oils Using Near Critical Solvents. *Ind. Eng. Chem. Res.* **2000**, *39*, 3024.

(31) Espinosa, S.; Diaz, S.; Brignole, E. A. Optimal Design of Supercritical Fluid Processes. *Comput. Chem. Eng.* **2000**, *24* (2/7), 1301.

(32) Skjold-Jørgensen, S. Gas Solubility Calculations. II. Application of a New Group-Contribution Equation of State. *Fluid Phase Equilibr.* **1984**, *16*, 317.

(33) Skjold-Jørgensen, S. Group Contribution Equation of State (GC-EOS): A Predictive Method for Phase Equilibrium Computations over Wide Ranges of Temperatures and Pressures up to 30 MPa. *Ind. Eng. Chem. Res.* **1988**, *27*, 110.

(34) Brignole, E. A.; Andersen, P. M.; Fredenslund, Aa. Super-critical Fluid Extraction of Alcohols from Water. *Ind. Eng. Chem. Res.* **1987**, *26*, 254.

(35) Brignole, E. A.; Skjold-Jørgensen, S.; Fredenslund, Aa. Application of the Group Contribution Equation of State to Supercritical Fluid Extraction. In *Supercritical Fluid Technology*; Penninger, Radosz, McHugh, and Krukonis, Eds.; Elsevier: Amsterdam, 1984; 87.

(36) Bottini, S.; Fornari, T.; Brignole, E. A. Phase Equilibrium Modeling of Triglycerides with Near Critical Solvents. *Fluid Phase Equilibr.* **1999**, *158*, 211.

(37) Espinosa, S.; Bermúdez, A.; Foco, G.; Fornari, T. Revision and Extension of The Group Contribution Equation of State to New Solvent Groups and Higher Molecular Weight Alkanes. *Fluid Phase Equilibr.* **2000**, *172* (2), 129.

(38) Fredenslund, Aa.; Gmehling, J.; Rassmusen, P. *Vapor-Liquid Equilibrium Using UNIFAC*; Elsevier Scientific Publishing Co.: Amsterdam, 1977.

(39) Joback, K. G.; Reid, R. C. Estimation of Pure-Component Properties from Group Contributions. *Chem. Eng. Commun.* **1983**, *57*, 233.

(40) Meissner, H. P. Critical Constants from Parachor and Molar Refraction. *Chem. Eng. Prog.* **1949**, *45*, 149.

(41) Inomata, H.; Kondo, T.; Hirohama, S.; Arai, K.; Suzuki, Y.; Konno, M. Vapor-Liquid Equilibria for Binary Mixtures of Carbon Dioxide and Fatty Acid Methyl Esters. *Fluid Phase Equilibr.* **1989**, *46*, 41.

(42) Bharath, R.; Inomata, H.; Arai, K.; Shoji, K.; Noguchi, Y. Vapor-Liquid Equilibria for Binary Mixtures of Carbon Dioxide and Fatty Acid Ethyl Esters. *Fluid Phase Equilibr.* **1989**, *50*, 315.

(43) Michelsen, M. L. The Isothermal Flash Problem. Part II: Phase Split Calculations. *Fluid Phase Equilibr.* **1982**, *9*, 21.

(44) Biegler, L. T.; Cuthrell, J. E. Improved Infeasible Path Optimization for Sequential Modular Simulators II: The Optimization Algorithm. *Comput. Chem. Eng.* **1985**, *9*, 257.